

CoDe-NeRF: Neural Rendering via Dynamic Coefficient Decomposition

Wenpeng Xing¹, Jie Chen², Zaifeng Yang³, Tiancheng Zhao⁴, Gaolei Li⁵, Changting Lin⁴, Yike Guo⁶, Meng Han¹

¹Zhejiang University ²Hong Kong Baptist University ³A*STAR, Singapore ⁴Binjiang Institute of Zhejiang University
⁵Shanghai Jiao Tong University ⁶Hong Kong University of Science and Technology

Abstract

Neural Radiance Fields (NeRF) have shown impressive performance in novel view synthesis, but challenges remain in rendering scenes with complex specular reflections and highlights. Existing approaches may produce blurry reflections due to entanglement between lighting and material properties, or encounter optimization instability when relying on physically-based inverse rendering. In this work, we present a neural rendering framework based on dynamic coefficient decomposition, aiming to improve the modeling of view-dependent appearance. Our approach decomposes complex appearance into a shared, static neural basis that encodes intrinsic material properties, and a set of dynamic coefficients generated by a Coefficient Network conditioned on view and illumination. A Dynamic Radiance Integrator then combines these components to synthesize the final radiance. Experimental results on several challenging benchmarks suggest that our method can produce sharper and more realistic specular highlights compared to existing techniques. We hope that this decomposition paradigm can provide a flexible and effective direction for modeling complex appearance in neural scene representations.

Introduction

Creating photorealistic, freely-navigable 3D scenes from a sparse set of 2D images is a fundamental challenge in computer graphics and vision, with critical applications in virtual reality (VR), augmented reality (AR), and digital twins. The advent of Neural Radiance Fields (NeRF) and its successors has revolutionized high-quality novel view synthesis by representing scenes as differentiable volumetric functions. However, while these methods excel at rendering diffuse or Lambertian surfaces, they still face significant challenges with the glossy or non-Lambertian surfaces ubiquitous in the real world, which exhibit complex highlights and specular reflections. These high-frequency, view-dependent effects demand a highly expressive model to be captured accurately, a weak point for many current leading methods.

Existing approaches have largely followed two paths to address this problem, each with its own limitations. The first category of methods, including TensoRF and 3D Gaussian Splatting (3DGS), focuses on improving the training and rendering efficiency of NeRF. Despite their remarkable success in speed, they often "bake" material and illumination

effects into a unified appearance representation. This entangled representation hinders their ability to render sharp, dynamically changing specular highlights, often resulting in blurry or view-inconsistent artifacts. The second category attempts to disentangle the physical properties of the scene via neural inverse rendering, for instance, by decomposing appearance into diffuse and specular components based on physical BRDF models. However, these methods often rely on complex optimization processes that are prone to unstable local minima, leading to ambiguous decompositions of material and light, and typically require strong geometric or illumination priors.

To overcome these limitations, we propose in this paper a novel neural rendering framework centered on a dynamic coefficient decomposition. Our core idea is to break down the complex task of modeling view-dependent appearance into two parts: a static, shared neural basis that represents the scene's intrinsic material properties, and a set of dynamic coefficients that adaptively change based on the viewing direction and illumination conditions. As illustrated in Figure 1, we design a Coefficient Network to generate these dynamic coefficients, which are then non-linearly combined with the basis by a Dynamic Radiance Integrator to synthesize the final color. This design avoids the rigid constraints and optimization challenges of traditional physical models, while being more expressive than simple linear models, thus enabling the efficient and high-fidelity rendering of sharp, detailed specular effects.

Our main contributions can be summarized as follows:

- We propose a novel dynamic coefficient decomposition framework, which provides a powerful and flexible paradigm for modeling complex view-dependent effects by combining a static neural basis with dynamic modulating coefficients.
- We design an effective Coefficient Network that leverages a FiLM-like affine transformation mechanism to generate coefficients, enabling the precise capture of appearance changes caused by view and illumination variations.
- Through extensive experiments on multiple challenging benchmarks, we demonstrate that our method achieves state-of-the-art performance in rendering glossy and reflective scenes, significantly outperforming prior meth-

ods in both qualitative and quantitative comparisons.

Related work

Neural Representations for Novel View Synthesis

Novel View Synthesis (NVS) aims to generate images of a scene from unobserved viewpoints, given a set of known images. Traditional methods heavily rely on explicit 3D geometry obtained from Multi-View Stereo (MVS) (Schönberger et al. 2016) or Photometric Stereo (PS) (Chen, Han, and Wong 2018), and synthesize new views by warping pixels between views. However, these methods often falter when dealing with specular reflections or textureless regions due to inaccurate depth estimation. Light field methods (Xing et al. 2022) enable high-quality interpolation within small baselines but struggle to support free-viewpoint rendering over large baselines.

Recent years have seen a breakthrough with implicit neural representations, most notably Neural Radiance Fields (NeRF) (Mildenhall et al. 2020). NeRF maps a 3D coordinate and a 2D viewing direction to a volumetric density and color using a multilayer perceptron (MLP), and leverages a differentiable volumetric rendering equation for end-to-end optimization. This approach has achieved unprecedented photorealistic rendering quality. However, the original NeRF suffers from several limitations, including slow training and rendering speeds, poor generalization, and insufficient capacity to model view-dependent effects like specular highlights.

To address the efficiency bottleneck, the research community has proposed various acceleration strategies. Some works employ explicit data structures like sparse voxel grids (Fridovich-Keil et al. 2022; Sun, Sun, and Chen 2022), or replace the implicit MLP with highly-efficient queryable feature fields via tensor decompositions (Chen et al. 2022; Fridovich-Keil et al. 2023), significantly reducing training time. Among these, TensorRF (Chen et al. 2022) models the scene using tensor factorization, striking a favorable balance between efficiency and quality. More recently, 3D Gaussian Splatting (3DGS) (Kerbl et al. 2023) proposes using 3D Gaussians as an explicit scene representation, enabling real-time, high-quality rendering. However, it can introduce artifacts when rendering complex reflections and dense scenes (Kwon et al. 2025). Despite these advances in speed and quality, most of these methods still entangle illumination and material properties, limiting their performance in scenes with complex lighting and shiny materials.

Relightable and Reflective Scene Modeling

To more realistically render shiny and reflective scenes, the core challenge lies in disentangling the scene’s intrinsic properties (e.g., material, geometry) from extrinsic illumination—a process often referred to as neural inverse rendering. Early works like NeRF-W (Martin-Brualla et al. 2021) introduced transient latent codes for each image to handle dynamic objects and lighting variations, but this acts as a non-physical correction and lacks a true decoupling of scene properties.

To achieve a more physically-accurate decomposition, subsequent works have shifted towards explicitly modeling materials and illumination. These methods typically decompose the scene’s radiance into diffuse and specular components. For instance, Ref-NeRF (Verbin et al. 2022) introduced feature queries along the reflection direction and regularization on surface normals, significantly improving its ability to model specular highlights. PhysSG (Zhang et al. 2021) and NeRO (Liu et al. 2023) go a step further by integrating physically-based rendering (PBR) models, such as the Bidirectional Reflectance Distribution Function (BRDF), into the neural field, while simultaneously predicting spatially-varying material parameters (e.g., albedo, roughness, metallic) and the environmental illumination. TensoIR (Jin et al. 2023) combines this idea with tensor factorization for efficient inverse rendering. However, these methods often rely on complex multi-stage optimization pipelines or strong priors (e.g., precise camera poses, light probes) and are prone to getting trapped in local minima during optimization, leading to an ambiguous decomposition of material and illumination.

In contrast to the works above, our method effectively captures complex view- and illumination-dependent effects through a dynamic, coefficient-driven decomposition. We neither rely on complex physical BRDF models and their unstable inverse optimization, nor are we constrained by the linear expressiveness of traditional basis learning. Through a non-linear fusion of adaptive coefficients and invariant neural bases, our method achieves high-fidelity rendering of specular reflections and highlights at a low computational overhead, without requiring dense views or additional priors, surpassing baseline models such as NeRF, TensorRF, and 3DGS in visual quality.

Preliminaries

Tensorial Radiance Fields

TensorRF (Chen et al. 2022) proposes a compact volumetric representation using vector-matrix (VM) decomposition. For a spatial point $x = (X, Y, Z)$ in volume \mathcal{V} , density features $\mathcal{T}_\sigma(x)$ and appearance features $\mathcal{T}_c(x)$ are queried, supporting efficient gradient propagation during training.

The radiance field tensor $\mathcal{T}_{\sigma,c}$ is factorized as a sum of outer products:

$$\mathcal{T}_{\sigma,c} = \sum_{r=1}^R \sum_{m \in \{X,Y,Z\}} \mathbf{v}_r^m \otimes \mathbf{M}_r^{\{X,Y,Z\} \setminus m}, \quad (1)$$

where \otimes is the outer product, and R is the decomposition rank, enabling low-memory storage and computation. Features at x are reconstructed via:

$$\mathcal{T}_{\sigma,c}(x) = \sum_{r=1}^{R_{\sigma,c}} \sum_{m \in \{X,Y,Z\}} \mathcal{A}_r^m(x), \quad (2)$$

where $\mathcal{A}_r^m(x)$ is the mode-specific component along axis m . Related work, such as K -Planes (Fridovich-Keil et al. 2023), extends this to planar factorization for dynamic scenes.

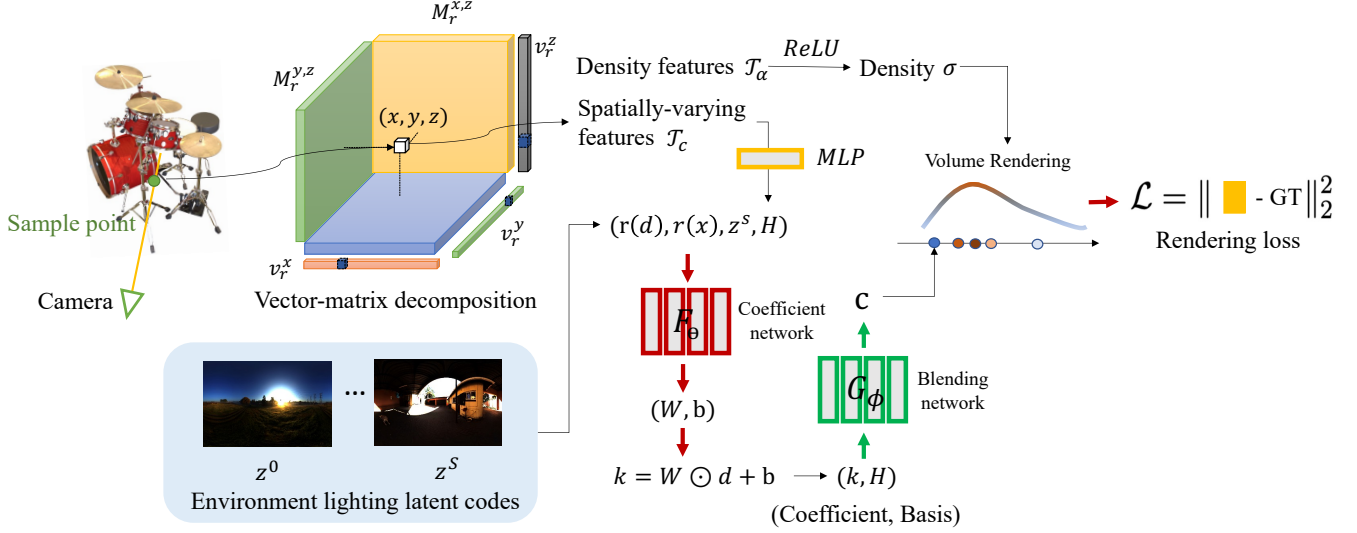


Figure 1: Overall pipeline of our method, centered on dynamic coefficient decomposition. This approach decomposes scene appearance into a static neural basis H (encoding material) and a set of dynamic coefficients k (encoding view and light). A Coefficient Network F_θ generates k , which are then non-linearly combined with H by a Dynamic Radiance Integrator G_ϕ to produce the final color. This disentangled design enables efficient, high-fidelity rendering of complex reflections.

Novel views are synthesized using differentiable volume rendering (Mildenhall et al. 2020), integrating radiance along camera rays:

$$\mathbf{C} = \sum_{x=1}^X T_x (1 - \exp(-\sigma_x \Delta_x)) L_o(x, d), \quad (3)$$

$$T_x = \exp\left(-\sum_{j=1}^{x-1} \sigma_j \Delta_j\right), \quad (4)$$

where $\sigma_x = \text{ReLU}(\mathcal{T}_\sigma(x))$ is the density, Δ_x is the step size, and $L_o(x, d)$ is the view-dependent color from $\mathcal{T}_c(x)$.

Proposed Method

Overview

We propose a novel framework for novel view synthesis that redefines the modeling of view- and illumination-dependent effects through a dynamic coefficient decomposition. Our core innovation lies in a coefficient network F_θ that adaptively generates view-conditioned coefficients k , enabling precise capture of complex specular reflections and lighting variations from multi-view images under consistent lighting $\{\mathcal{I}_i\}_{i=1}^N$ or diverse conditions $\{\mathcal{I}_i^s\}_{i=1, s=1}^{N, S}$. This approach, depicted in Figure 1, achieves unparalleled rendering fidelity by blending these coefficients with a shared neural basis, advancing beyond traditional Neural Radiance Fields (Mildenhall et al. 2020).

Specifically, our method represents the scene via a volumetric field \mathcal{V} , where each point $x \in \mathbb{R}^3$ is associated with:

- Density features $\mathcal{T}_\sigma(x) \in \mathbb{R}^{R_\sigma^1 + R_\sigma^2 + R_\sigma^3}$, governing geometry,

- Appearance features $\mathcal{T}_c(x) \in \mathbb{R}^{R_c^1 + R_c^2 + R_c^3}$, encoding material properties.

These appearance features are projected into a compact set of view-agnostic neural bases $H = \{h_n\}_{n=1}^{N_p}$, which encapsulate reusable reflection patterns. The coefficient network F_θ processes $\mathcal{T}_c(x)$, viewing direction d , and a learnable illumination embedding $z^s \in \mathbb{R}^D$ to produce coefficients k , which are blended with H via a Dynamic Radiance Integrator G_ϕ to yield outgoing radiance $L_o(x, d, z^s)$ for volume rendering. Auxiliary illumination embeddings $Z = \{z^s\}_{s=1}^S$ enhance flexibility across lighting conditions.

In summary, our framework synergizes the coefficient network F_θ for dynamic view-light modulation, the neural basis H for reusable reflection patterns, the Dynamic Radiance Integrator G_ϕ for non-linear radiance synthesis, and illumination embeddings Z for versatile lighting adaptation. This integrated design enables high-fidelity rendering for applications like immersive VR.

Neural Approximation of Physics-Driven Rendering

Traditional rendering employs image-based lighting (IBL) to model surface appearance, formalized as:

$$L_o(x, d) = \int_{\Omega} f_r(x, \omega_i, d) L_i(x, \omega_i) (\omega_i \cdot \mathbf{n}) d\omega_i, \quad (5)$$

where $L_o(x, d)$ is the outgoing radiance, f_r the BRDF, \mathbf{n} the surface normal, and ω_i the incoming light direction. This integral, while accurate, demands intensive computation due to dense sampling across the light field.

Such computational complexity limits real-time applications. Previous methods like Neural-PIL (Boss et al. 2021b)

mitigate this by precomputing shadowing and Fresnel effects into textures, yet incur prolonged training times. Similarly, Spherical Gaussians (Boss et al. 2021a; Gardner et al. 2019; Li et al. 2020) often fail to capture high-frequency specular details (Munkberg et al. 2022). To address these shortcomings, we propose a neural approximation that replaces explicit integration with a dynamic coefficient-driven decomposition. Specifically, the decomposition consists of the following stages:

1. **Dynamic Coefficient Prediction.** The coefficient network F_θ generates view- and lighting-adaptive coefficients k :

$$F_\theta : (r(x), r(d), z^s, H) \rightarrow k, \quad (6)$$

where $r(\cdot)$ denotes positional encoding (Mildenhall et al. 2020), and $H = \{h_n\}_{n=1}^{N_p}$ is derived from appearance features:

$$H = \mathcal{W} \cdot \mathcal{T}_c, \quad \mathcal{W} \in \mathbb{R}^{(R_c^1 + R_c^2 + R_c^3) \times N_p}. \quad (7)$$

This stage leverages view direction d to modulate reflection patterns with high precision.

2. **Neural Blending of Reflectance Patterns.** The Dynamic Radiance Integrator G_ϕ fuses k and H into radiance L_o :

$$G_\phi : (k, H) \rightarrow L_o. \quad (8)$$

This non-linear blending captures complex effects, surpassing static sums. The final radiance is:

$$L_o(x, d) = G_\phi(F_\theta(r(d), r(x), z^s, H), H). \quad (9)$$

3. **Illumination Embedding for Flexibility.** To support varying lighting, we introduce learnable codes $z^s \in \mathbb{R}^D$, optimized jointly:

$$z^s \approx \int_{\Omega} L_i(x, \omega_i)(\omega_i \cdot \mathbf{n}) d\omega_i. \quad (10)$$

Initialized normally, z^s ensures smooth interpolation across conditions, omitted in single-illumination cases for efficiency.

This illumination embedding complements our core innovation: a dynamic coefficient decomposition that drives view- and lighting-dependent rendering. By integrating z^s with appearance features and view directions, our framework reformulates the image-based lighting model (Eq. 5) into a neural approximation, expressed as:

$$L_o(x, d) = G_\phi(F_\theta(r(d), r(x), z^s, H), H), \quad (11)$$

where F_θ generates adaptive coefficients k , and G_ϕ blends them with neural bases H to produce outgoing radiance L_o . This decomposition enables high-fidelity rendering of specular effects, seamlessly bridging physical accuracy with computational efficiency. We next detail the coefficient network F_θ , which underpins this process by dynamically modulating view-dependent reflection patterns.

Coefficient Network The coefficient network F_θ , implemented as a multi-layer perceptron (MLP) with dynamic factorization layers, combines point coordinates x , viewing direction d , illumination embedding z^s , and neural basis H to generate adaptive coefficients k . Inspired by factorized radiance field designs, this network addresses the conditioning challenge (Dumoulin et al. 2018) by decomposing inputs into structured components: x and H represent spatial-material features, d modulates view-dependent effects, and z^s accounts for lighting variations via tensor contraction. The output k serves to adaptively weight reflection patterns in H , enabling efficient rendering through low-rank approximation.

To better capture view-dependent effects, we adopt an extended feature-wise linear modulation (FiLM) mechanism with a multi-basis formulation. For a given scene point x , with fixed material basis H and illumination z^s , the directional input d is modulated as:

$$k = W_x \odot d + b_x, \quad (12)$$

where \odot denotes the Hadamard product, $W_x \in \mathbb{R}^{N_w \times 3}$ is a learned weight matrix, and $b_x \in \mathbb{R}^{N_w}$ is a bias term. This affine transformation is further constrained by BRDF-inspired priors to improve physical plausibility, particularly in modeling specular highlights and high-frequency details.

Compared to conventional conditioning strategies (Chan et al. 2021; Perez et al. 2018; Dumoulin et al. 2018; Attal et al. 2022), our design offers the following advantages:

- **Structured Input Decomposition:** The use of low-rank factorization allows stable and interpretable modulation of spatial, directional, and lighting inputs.
- **Improved Directional Conditioning:** The FiLM-based formulation helps preserve directional information d under varying lighting z^s , reducing signal entanglement.

This modular and decomposition-aware design of F_θ contributes to the overall effectiveness of our dynamic radiance synthesis framework.

Dynamic Radiance Integrator The dynamic radiance integrator network G_ϕ , implemented as a multi-layer perceptron (MLP), approximates the integral form of image-based rendering (IBR) equations, such as the bidirectional reflectance distribution function (BRDF) integral in Eq. (5). This network dynamically fuses adaptive coefficients k with the neural basis H to synthesize outgoing radiance $L_o(x, d, z^s)$, enabling high-fidelity capture of view- and illumination-dependent effects, such as specular reflections.

To effectively approximate the complex, non-linear behavior of real-world reflectance, we adopt MLPs due to their superior expressiveness and flexibility. Unlike static weighted sums, MLPs can model high-order interactions between k and H , outperforming static weighted sums by better approximating non-linear reflectance patterns. Mathematically, the network simulates the IBR integral through a decomposed representation. The traditional BRDF integral is:

$$L_o(x, d) = \int_{\Omega} f_r(x, \omega_i, d) L_i(x, \omega_i)(\omega_i \cdot \mathbf{n}) d\omega_i. \quad (13)$$

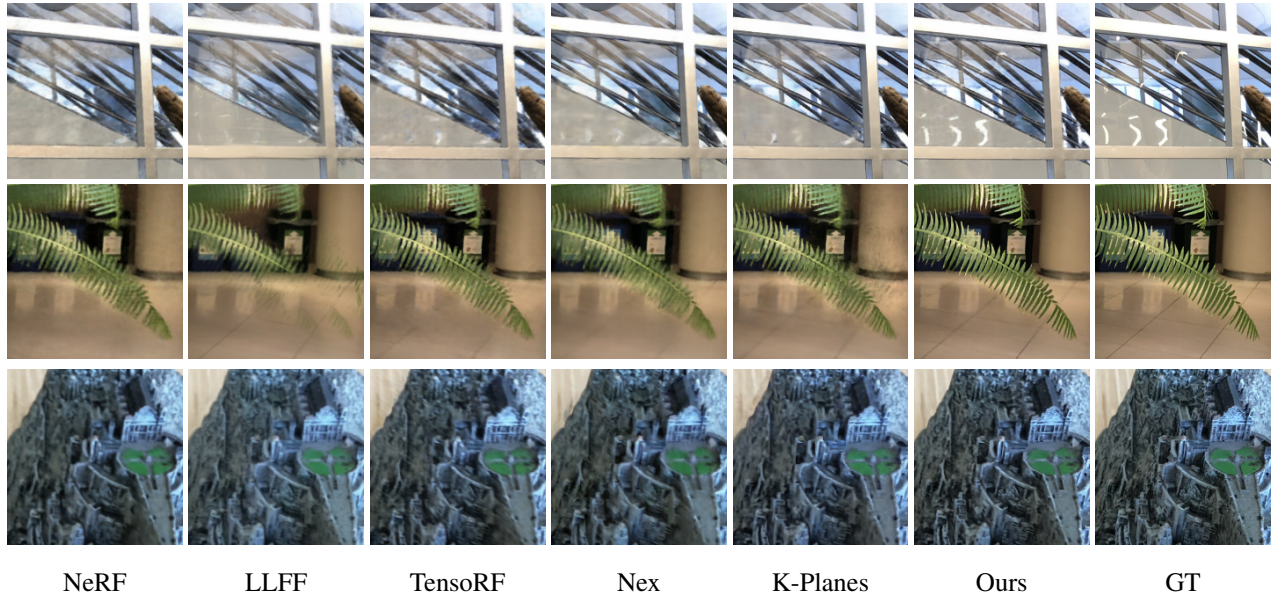


Figure 2: Qualitative comparisons on test views from the Forward-Facing dataset. For each scene (Horns, Fern, Fortress), the full image rendered by our method is shown on the left, followed by close-up crops from various baseline methods and the ground truth.

By decomposing f_r into coefficients k (generated by F_θ) and basis H , the approximation becomes:

$$L_o(x, d) \approx G_\phi(k, H) = \sigma(W_2 \cdot \sigma(W_1 \cdot [k; H] + b_1) + b_2), \quad (14)$$

where σ is an activation function (e.g., ReLU), and W_1, W_2, b_1, b_2 are learnable parameters. This non-linear fusion captures high-order interactions. Specifically, the MLP concatenates the view-invariant neural basis H and coefficients k as input, producing view- and illumination-dependent radiance L_o as output, as in Eq. (8).

In collaboration with upstream components, G_ϕ integrates seamlessly: coefficients k from F_θ modulate dynamic factors, while H provides reusable reflectance patterns, and illumination embeddings z^s ensure adaptability across lighting conditions. Finally, volume rendering via Eq. (4) aggregates L_o along rays to yield pixel colors C , achieving photorealistic novel views with computational efficiency.

Loss Function

The tensor features $\mathcal{T}_{c,\sigma}$ and the illumination latent codes $\{z^s \in \mathbb{R}^D\}_{s=1}^S$ are jointly optimized by minimizing a combination of an L2 photometric rendering loss and regularization terms, as inspired by tensorial radiance field methods (Chen et al. 2022). This objective is formulated as:

$$\mathcal{L} = \|\mathbf{C} - \bar{\mathbf{C}}\|_2^2 + \lambda \cdot \mathcal{L}_{\text{reg}}, \quad (15)$$

where $\bar{\mathbf{C}}$ denotes the ground-truth pixel color, and λ is a hyperparameter controlling the strength of the regularization term \mathcal{L}_{reg} .

To promote spatial smoothness in the appearance features \mathcal{T}_c and density features \mathcal{T}_σ , we employ a Total Variation

(TV) regularization loss on the vector-matrix decomposition parameters \mathbf{V}, \mathbf{M} . This regularization mitigates artifacts in sparsely sampled regions and enhances reconstruction stability. The TV loss is expressed as:

$$\mathcal{L}_{\text{reg}} = \frac{1}{P} \sum \left(\lambda_1 \sqrt{\Delta^2 \mathbf{V}} + \lambda_2 \sqrt{\Delta^2 \mathbf{M}} \right), \quad (16)$$

where P is the total number of parameters, Δ^2 represents the squared differences between neighboring parameters, and λ_1, λ_2 are weighting hyperparameters.

Experiment Setup

Implementation Details Our method is implemented in PyTorch 1.12. We set an alpha masking threshold of 0.01 to localize surface points, updating the mask at iterations [1000, 2000, 3000, 4000, 5000, 6000, 7000] to exclude empty regions during training. We employ 3-level tensor decompositions for density and appearance features, with channel dimensions [16, 16, 16] for $\{R_\sigma^1, R_\sigma^2, R_\sigma^3\}$ and [48, 48, 48] for $\{R_c^1, R_c^2, R_c^3\}$. Positional encodings for 3D points and view directions use 2 frequency levels. The illumination embedding dimension D and FiLM modulation dimension N_w are both set to 32, with 16 neural basis functions ($N_p = 16$). The coefficient network F_θ is an 8-layer MLP with 256 hidden units and leaky ReLU activations (Xu et al. 2015). The dynamic radiance integrator G_ϕ is a 3-layer MLP with 128 hidden units and ReLU activations. Training runs for 100k iterations with a batch size of 5,000 and an initial learning rate of 0.02. On a single NVIDIA A100 GPU, training a NeRF-Synthetic scene for 10k iterations takes approximately 2 hours.

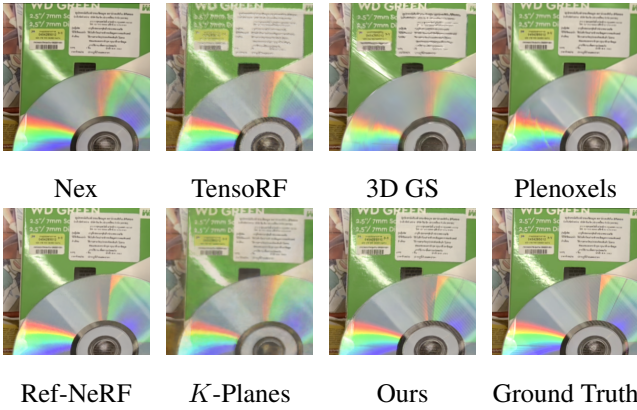


Figure 3: Qualitative comparison on the *CD* scene from the Shiny dataset (Wizadwongsa et al. 2021). Our method better preserves specular highlights and structural details compared to prior methods.

Datasets We evaluate our method on three established benchmarks: NeRF-Synthetic (Mildenhall et al. 2020), Forward-Facing (Mildenhall et al. 2019), and Shiny (Wizadwongsa et al. 2021).

Competing Methods We compare our method against state-of-the-art neural rendering baselines, grouped into four categories: NeRF variants, voxel/grid-based methods, tensor decomposition approaches, and efficient/explicit representations, plus one additional method. NeRF Variants: NeRF (Mildenhall et al. 2020), Ref-NeRF (Verbin et al. 2022), Tetra-NeRF (Kulhanek and Sattler 2023), Point-NeRF (Xu et al. 2022), SRN (Sitzmann, Zollhöfer, and Wetzstein 2019). Voxel/Grid-Based: Plenoxels (Fridovich-Keil et al. 2022), DVGO (Sun, Sun, and Chen 2022), PlenOctrees (Yu et al. 2021). Tensor Decomposition: TensoRF (VM-192) (Chen et al. 2022), K-Planes (Fridovich-Keil et al. 2023). Efficient/Explicit Representations: Instant-NGP (Müller et al. 2022), 3D Gaussian Splatting (Kerbl et al. 2023), Nex (Wizadwongsa et al. 2021), LLFF (Mildenhall et al. 2019).

Most methods were re-trained under consistent settings for fair comparison, with original results used where applicable.

Experiment Results

Quantitative Results

Tables 1 present average quantitative results on NeRF-Synthetic and Forward-Facing datasets under consistent illumination. Our method achieves top performance, surpassing NeRF by 3.17 dB (PSNR) on NeRF-Synthetic and 6.83 dB on Forward-Facing, with superior SSIM and LPIPS scores, indicating enhanced structural and perceptual quality.

Table 2 shows results for dense-view training on the *materials* scene from NeRF-Synthetic with 100, 200, and 300 views. Our method consistently outperforms baselines, with PSNR improvements of 1.19–3.21 dB over TensoRF, the closest competitor. Notably, our approach scales effectively

with view count, unlike 3D GS, which suffers from popping artifacts due to view-dependent effects.

Table 1: Quantitative comparison on NeRF-Synthetic (Mildenhall et al. 2020) and Forward-Facing (Mildenhall et al. 2019). Best results in **bold**.

Method	NeRF-Synthetic			Forward-Facing		
	PSNR \uparrow	SSIM \uparrow	LPIPS \downarrow	PSNR \uparrow	SSIM \uparrow	LPIPS \downarrow
SRN	22.26	0.846	0.170	–	–	–
NeRF	31.01	0.947	0.081	26.50	0.811	0.250
LLFF	–	–	–	24.41	0.863	0.211
PlenOctrees	31.71	0.958	0.053	–	–	–
Plenoxels	31.71	0.958	0.049	26.29	0.839	0.210
DVGO	31.95	0.957	0.053	–	–	–
TensoRF	32.39	0.957	0.057	26.51	0.832	0.217
Instant-NGP	27.22	–	0.206	–	–	–
K-Planes	32.37	0.962	0.150	26.80	0.846	0.193
3D GS	32.84	0.962	0.042	–	–	–
Tetra-NeRF	32.53	0.952	0.041	–	–	–
Point-NeRF	33.31	0.968	0.049	–	–	–
Ref-NeRF	33.99	0.926	0.038	–	–	–
Nex	–	–	–	27.26	0.904	0.178
Ours	34.18	0.970	0.037	33.33	0.945	0.117

Qualitative Results

Figure 2 and Figure 3 showcase qualitative improvements in rendering fine textures (*Horn, Fortress, Ferns*) and reflective surfaces (*Materials, Drums, Ficus, CDs, book covers*), validating our method’s ability to model geometry and appearance synergistically.

Ablation Study

Effect of Dynamic Decomposition. In variant (a), we remove our entire dynamic coefficient decomposition module (including F_θ , H , and G_ϕ) and replace it with a standard MLP appearance head that maps appearance features and view direction directly to color. As shown in Table 3, this results in the most significant performance drop among all ablations (over 3dB in PSNR and a nearly 4x worse LPIPS score). Qualitatively, this variant fails to render sharp, view-consistent specular highlights, producing blurry or smeared reflections instead. This strongly confirms that our decomposition framework is fundamental to successfully disentangling material properties from view-dependent effects for high-fidelity rendering.

Analysis of the Blending Mechanism. For variant (b), we replace the non-linear Dynamic Radiance Integrator G_ϕ with a simple linear operation (a dot product between coefficients and bases). While this model retains the decomposition structure, its performance still drops noticeably, especially on the perceptual LPIPS metric. The rendered results show highlights that, while present, appear dull and lack nuance, failing to capture the rich details arising from complex light-material interactions. This demonstrates that non-linear blending is crucial for synthesizing photorealistic radiance.

Table 2: Quantitative results on *materials* scene (NeRF-Synthetic) with dense views (Mildenhall et al. 2020).

#Views	Method	PSNR \uparrow	SSIM \uparrow	LPIPS \downarrow
100	TensoRF	31.42	0.961	0.020
	DVGO	30.60	0.959	0.049
	3D GS	30.49	0.960	0.037
	<i>K</i> -Planes	29.46	0.949	0.064
	Instant-NGP	25.27	–	0.303
	Plenoxels	29.13	0.949	0.057
	Ours	32.61	0.970	0.015
200	TensoRF	32.68	0.969	0.016
	DVGO	31.63	0.967	0.045
	3D GS	27.96	0.936	0.088
	<i>K</i> -Planes	30.75	0.961	0.053
	Instant-NGP	27.65	–	0.202
	Plenoxels	30.99	0.967	0.039
	Ours	34.77	0.979	0.010
300	TensoRF	33.06	0.971	0.015
	DVGO	31.96	0.968	0.043
	3D GS	27.95	0.936	0.088
	<i>K</i> -Planes	30.92	0.962	0.052
	Instant-NGP	28.12	–	0.167
	Plenoxels	31.22	0.969	0.038
	Ours	36.27	0.983	0.009

Table 3: Quantitative results for the ablation study on core components. Best results are in **bold**.

#	Model Variant	PSNR \uparrow	SSIM \uparrow	LPIPS \downarrow
	Ours (Full Model)	32.54	0.968	0.041
(a)	w/o Decomposition	29.13	0.925	0.158
(b)	w/o Dynamic Radiance Integrator	31.02	0.951	0.083
(c)	w/o FiLM in F_θ	31.78	0.959	0.065
(d)	w/o Neural Basis	32.21	0.964	0.052

Analysis of the Coefficient Network Design. In variant (c), we replace the FiLM-like affine transform in the Coefficient Network F_θ with simple feature concatenation. The results show a measurable decrease in performance. We posit that simple concatenation dilutes the view-direction signal, making it difficult for the network to learn the high-frequency details caused by subtle changes in viewpoint. Our FiLM-inspired design, however, explicitly uses the view direction to modulate other features, enabling more precise control over specular effects.

Effect of the Neural Basis. In variant (d), we remove the projection to a neural basis and instead feed the higher-dimensional raw appearance features directly into the Dynamic Radiance Integrator. Interestingly, this variant shows only a slight performance drop. However, this comes at the cost of model efficiency and parameter count. The Dynamic Radiance Integrator must process a much larger input, increasing its complexity. More importantly, distilling features into a compact, shared basis forces the model to learn a reusable dictionary of reflectance patterns, which can lead to better generalization and interpretability. Thus, the neural

basis design is key to achieving an optimal balance between performance and efficiency.

Analysis of Hyperparameters

We also analyze the impact of the number of neural bases, N_p , on the model’s expressive power.

Table 4: Impact of the number of neural bases (N_p). Too few bases limit the model’s expressiveness, while too many can lead to diminishing returns and potential overfitting.

N_p (Number of Bases)	PSNR \uparrow
4	31.26
8	32.11
16	32.54
32	32.57

As shown in Table 4, performance improves significantly as N_p increases from 4 to 16, indicating that more bases allow the model to represent richer material reflectance patterns. However, the improvement becomes marginal when increasing from 16 to 32. This suggests that 16 bases are sufficient for the test scenes, and more may introduce a risk of overfitting and unnecessary computational overhead. We therefore use $N_p = 16$ as our default configuration in all main experiments.

Conclusion

In this paper, we introduced a novel neural rendering framework based on dynamic coefficient decomposition to address the challenge of rendering highly reflective scenes. Our method models complex appearance by decoupling a static, shared neural basis representing material properties from dynamic coefficients that are generated by a Coefficient Network to adapt to view and illumination. Experiments demonstrate that this approach achieves state-of-the-art quality and quantitative performance, particularly in rendering specular highlights and other view-dependent effects.

While effective, our method’s latent-based illumination model is limited in handling local lighting effects like cast shadows, and it does not yet yield editable physical material parameters. Key directions for future work therefore include integrating more structured lighting representations for photorealistic relighting, and extending the framework to predict editable material properties. We believe the decomposition paradigm presented here offers a promising new direction for neural rendering.

Limitations

Our primary limitations are twofold. First, the latent-based illumination model prevents photorealistic relighting with local effects such as cast shadows. Second, our framework does not disentangle explicit physical parameters, thus disallowing direct material editing.

References

- Attal, B.; Huang, J.-B.; Zollhöfer, M.; Kopf, J.; and Kim, C. 2022. Learning Neural Light Fields With Ray-Space Embedding. In *CVPR*, 19819–19829.
- Boss, M.; Braun, R.; Jampani, V.; Barron, J. T.; Liu, C.; and Lensch, H. 2021a. Nerd: Neural reflectance decomposition from image collections. In *ICCV*, 12684–12694.
- Boss, M.; Jampani, V.; Braun, R.; Liu, C.; Barron, J.; and Lensch, H. 2021b. Neural-pil: Neural pre-integrated lighting for reflectance decomposition. *Advances in Neural Information Processing Systems*, 34: 10691–10704.
- Chan, E. R.; Monteiro, M.; Kellnhofer, P.; Wu, J.; and Wetzstein, G. 2021. pi-gan: Periodic implicit generative adversarial networks for 3d-aware image synthesis. In *CVPR*, 5799–5809.
- Chen, A.; Xu, Z.; Geiger, A.; Yu, J.; and Su, H. 2022. TensorRF: Tensorial Radiance Fields. In *ECCV*, 333–350.
- Chen, G.; Han, K.; and Wong, K.-Y. K. 2018. PS-FCN: A flexible learning framework for photometric stereo. In *ECCV*, 3–18.
- Dumoulin, V.; Perez, E.; Schucher, N.; Strub, F.; Vries, H. d.; Courville, A.; and Bengio, Y. 2018. Feature-wise transformations. *Distill*, 3(7): e11.
- Fridovich-Keil, S.; Meanti, G.; Warburg, F. R.; Recht, B.; and Kanazawa, A. 2023. K-planes: Explicit radiance fields in space, time, and appearance. In *CVPR*, 12479–12488.
- Fridovich-Keil, S.; Yu, A.; Tancik, M.; Chen, Q.; Recht, B.; and Kanazawa, A. 2022. Plenoxels: Radiance Fields Without Neural Networks. In *CVPR*, 5501–5510.
- Gardner, M.-A.; Hold-Geoffroy, Y.; Sunkavalli, K.; Gagné, C.; and Lalonde, J.-F. 2019. Deep parametric indoor lighting estimation. In *ICCV*, 7175–7183.
- Jin, H.; Liu, I.; Xu, P.; Zhang, X.; Han, S.; Bi, S.; Zhou, X.; Xu, Z.; and Su, H. 2023. TensorIR: Tensorial Inverse Rendering. In *CVPR*.
- Kerbl, B.; Kopanas, G.; Leimkühler, T.; and Drettakis, G. 2023. 3D Gaussian Splatting for Real-Time Radiance Field Rendering. *ACM Transactions on Graphics*, 42(4).
- Kulhanek, J.; and Sattler, T. 2023. Tetra-nerf: Representing neural radiance fields using tetrahedra. In *ICCV*, 18458–18469.
- Kwon, W.; Sung, J.; Jeon, M.; Eom, C.; and Oh, J. 2025. R3eVision: A Survey on Robust Rendering, Restoration, and Enhancement for 3D Low-Level Vision. *arXiv preprint arXiv:2506.16262*.
- Li, Z.; Shafiei, M.; Ramamoorthi, R.; Sunkavalli, K.; and Chandraker, M. 2020. Inverse rendering for complex indoor scenes: Shape, spatially-varying lighting and svbrdf from a single image. In *CVPR*, 2475–2484.
- Liu, Y.; Wang, P.; Lin, C.; Long, X.; Wang, J.; Liu, L.; Komura, T.; and Wang, W. 2023. Nero: Neural geometry and brdf reconstruction of reflective objects from multiview images. *ACM Transactions on Graphics (ToG)*, 42(4): 1–22.
- Martin-Brualla, R.; Radwan, N.; Sajjadi, M. S.; Barron, J. T.; Dosovitskiy, A.; and Duckworth, D. 2021. Nerf in the wild: Neural radiance fields for unconstrained photo collections. In *Proceedings of the IEEE/CVF conference on computer vision and pattern recognition*, 7210–7219.
- Mildenhall, B.; Srinivasan, P. P.; Ortiz-Cayon, R.; Kalantari, N. K.; Ramamoorthi, R.; Ng, R.; and Kar, A. 2019. Local Light Field Fusion: Practical View Synthesis with Prescriptive Sampling Guidelines. *ACM Transactions on Graphics*, 38(4): 1–14.
- Mildenhall, B.; Srinivasan, P. P.; Tancik, M.; Barron, J. T.; Ramamoorthi, R.; and Ng, R. 2020. NeRF: Representing Scenes as Neural Radiance Fields for View Synthesis. In *ECCV*, 405–421.
- Müller, T.; Evans, A.; Schied, C.; and Keller, A. 2022. Instant Neural Graphics Primitives with a Multiresolution Hash Encoding. *ACM Transactions on Graphics*, 41(4): 102:1–102:15.
- Munkberg, J.; Hasselgren, J.; Shen, T.; Gao, J.; Chen, W.; Evans, A.; Müller, T.; and Fidler, S. 2022. Extracting Triangular 3D Models, Materials, and Lighting From Images. In *CVPR*, 8280–8290.
- Perez, E.; Strub, F.; De Vries, H.; Dumoulin, V.; and Courville, A. 2018. Film: Visual reasoning with a general conditioning layer. In *AAAI*, volume 32.
- Schönberger, J. L.; Zheng, E.; Pollefeys, M.; and Frahm, J.-M. 2016. Pixelwise View Selection for Unstructured Multi-View Stereo. In *ECCV*, 501–518.
- Sitzmann, V.; Zollhöfer, M.; and Wetzstein, G. 2019. Scene representation networks: Continuous 3D-structure-aware neural scene representations. In *Proc. Advances in Neural Information Processing Systems*, 1121–1132.
- Sun, C.; Sun, M.; and Chen, H.-T. 2022. Direct voxel grid optimization: Super-fast convergence for radiance fields reconstruction. In *CVPR*, 5459–5469.
- Verbin, D.; Hedman, P.; Mildenhall, B.; Zickler, T.; Barron, J. T.; and Srinivasan, P. P. 2022. Ref-nerf: Structured view-dependent appearance for neural radiance fields. In *CVPR*, 5481–5490.
- Wizadwongsa, S.; Phongthawee, P.; Yenphraphai, J.; and Suwajanakorn, S. 2021. Nex: Real-time view synthesis with neural basis expansion. In *CVPR*, 8534–8543.
- Xing, W.; Chen, J.; Yang, Z.; Wang, Q.; and Guo, Y. 2022. Scale-Consistent Fusion: from Heterogeneous Local Sampling to Global Immersive Rendering. *IEEE Transactions on Image Processing*.
- Xu, B.; Wang, N.; Chen, T.; and Li, M. 2015. Empirical evaluation of rectified activations in convolutional network. *arXiv preprint arXiv:1505.00853*.
- Xu, Q.; Xu, Z.; Philip, J.; Bi, S.; Shu, Z.; Sunkavalli, K.; and Neumann, U. 2022. Point-nerf: Point-based neural radiance fields. In *CVPR*, 5438–5448.
- Yu, A.; Li, R.; Tancik, M.; Li, H.; Ng, R.; and Kanazawa, A. 2021. Plenotrees for real-time rendering of neural radiance fields. In *ICCV*, 5752–5761.
- Zhang, K.; Luan, F.; Wang, Q.; Bala, K.; and Snavely, N. 2021. Physg: Inverse rendering with spherical gaussians for physics-based material editing and relighting. In *CVPR*, 5453–5462.